Slip rate and tremor genesis in Cascadia

Aaron G. Wech & Noel M. Bartlow

Abstract

At many plate boundaries, conditions in the transition zone between seismogenic and stable slip produce slow earthquakes. In the Cascadia subduction zone, these slow earthquakes are consistently observed as slow, aseismic slip on the plate interface accompanied by persistent tectonic tremor. However, not all slow slip at other plate boundaries coincides spatially and temporally with tremor, leaving the physics of tremor generation poorly understood. Here we analyze seismic, geodetic and borehole strainmeter data in Cascadia to observe for the first time a large, tremor-generating slow earthquake change from tremor-genic to silent and back again. The tremor falls silent at reduced slip speeds when the migrating slip front pauses as it loads the stronger adjacent fault segment to failure. The finding suggests that rheology and stress-regulated slip speed control tremor genesis, and the same section of fault can slip both with and without detectable tremor, limiting tremor's use as a proxy for slip.

Introduction

Slow earthquakes, where a fault interface can relieve stress in discrete, but stable episodes of slip, play a fundamental role in accommodating plate convergence in the transition zones of plate boundaries worldwide [*Schwartz and Rokosky*, 2007] These events typically occur adjacent to seismogenic parts of the same fault and may increase the stress on these locked regions with the potential to trigger large earthquakes as has been suggested for the Tohoku megathrust earthquake [*Ito et al.*, 2013; *Kato et al.*, 2012]. Monitoring where, when and how much slip occurs provides insight into the state of stress at the base of the seismogenic zone, improving long-term and time-dependent hazard assessments. In the Cascadia subduction zone, where the Juan de Fuca plate subducts beneath North America, slow earthquakes occur as repeating episodes of geodetically observed slow slip coincident with seismically observed tectonic tremor, together called episodic tremor and slip (ETS)

[*Rogers and Dragert*, 2003]. Though tremor only represents a tiny fraction of the total moment release [*Kao et al.*, 2010], detailed studies of the tremor source process [*Bostock et al.*, 2012; *Shelly et al.*, 2007; *Wech and Creager*, 2007] and the spatio-temporal correlation of slip and tremor [*Bartlow et al.*, 2011; *Hirose and Obara*, 2010] suggest that tremor is the seismic signature of slip at the fault interface. Thus the well-established correlation between tremor and slip in Cascadia enlists tremor as a powerful tool for mapping out slip distributions and cataloging slip history because of the higher spatial and temporal resolution of tremor observations, compared with direct geodetic observations of slip.

But these two phenomena do not always coincide. Strike slip boundaries show no surface deformation concurrent with deep tremor [*Shelly and Johnson*, 2011; *Wech et al.*, 2012], and there are a range of smaller tremor swarms that occur in Cascadia without any associated geodetic signal [*Wech et al.*, 2010]. These shorter duration swarms and tremor on strike-slip faults are interpreted to represent shear slip below the threshold for geodetic detection, but slip without tremor is less understood. Though not previously observed in Cascadia, some subduction zones have slow slip events that don't produce tremor. Slow slip beneath the Boso peninsula in Japan and offshore Cape Turnagain in New Zealand have no observed tremor but are accompanied by swarms of seismicity [*Ozawa et al.*, 2007; *Wallace et al.*, 2012]. Similarly, long-term slow slip events in Japan, New Zealand and Mexico have little to no accompanying tremor signals, or tremor and slip are not co-located [*Brudzinski et al.*, 2010; *Hirose et al.*, 2010; *Ide*, 2012]. Explanations for this diverse behavior range from differences in plate interface properties [*Peng and Gomberg*, 2010] to network limitations [*Wech et al.*, 2012]. In this study we control for both frictional properties and seismic network by using data from the same network to record a Cascadia ETS event that slipped both with and without tremor on the same fault patch, allowing a direct comparison of tremor-genic and tremorless slip.

Adjacent ETS events

We focus on tremor and slip activity in 2011 when two ETS events occurred within weeks and ~50 km of each other (Fig. 1). The central section of the Cascadia subduction zone, where ETS repeats every ~20 months [*Brudzinski and Allen*, 2007], ruptured first. On June 4, 2011, approximately 21 months after the 2009 ETS [*Bartlow et al.*, 2011], tremor and slip initiated at the downdip edge of the ETS zone in northern Oregon (Figs. 1 & 2), similar to previous ETS events [*Wech*, 2010]. Epicenters migrated updip over the next five days (Fig. S1) before partitioning and extending both north and south along strike. The southern tremor front stopped in central Oregon on June 15, but the northern front continued its ~8 km/day along strike migration 150 km before stopping in southern Washington on July 3 (Fig. 1).

Just 21 days later and ~50 km further north, tremor was detected beneath central Washington near the updip edge of the ETS zone on July 24. This tremor burst marked the beginning of the northern Cascadia ETS event, 10.5 months into its usual 13-16 month cycle [*Miller et al.*, 2002; *Rogers and Dragert*, 2003]. The tremor continued and migrated north along strike for the next 42 days before terminating beneath Vancouver Island (Fig. 1). Because slow slip has never been seen without tremor in Cascadia, to first order, this spatio-temporal gap in tremor would suggest an absence of slip as well. However, the relative timing and along-strike migration rate of the tremor epicenters in both events (Fig. 1) invites a causal connection between the events—perhaps tremorless slip continued in the gap between the two ETS events.

Tremorless slip

Tremor is routinely detected across the entire subduction zone using automated methods at the Pacific Northwest Seismic Network [*Wech*, 2010], but the inherent limitations of unchecked automation present numerous opportunities for false negative results. We therefore perform a manual tremor search by visually inspecting bandpass-filtered waveforms and envelopes of all available seismic data in southern Washington during the 3-week quiescence. We identify some continued minor

3

tremor on July 4 at the northern edge of the Oregon ETS event, but we otherwise find no evidence for undetected tremor. While visually apparent tremor can be ruled out, whether the low slip-speed slip is *truly* aseismic is difficult to definitively say. We were unable to identify clear tremor despite favorable noise levels during the gap (Fig. S2), but future studies using low-frequency earthquakes [*Shelly et al.*, 2007] could elucidate the presence or absence of a subtler seismic signature.

To investigate possible slip, we perform a 90-day time-dependent inversion of daily GPS solutions from the Pacific Northwest Geodetic Array. Following the approach of *Bartlow et al.* [2011], we invert these data using the Network Inversion Filter [*Segall and Matthews*, 1997] (NIF) to obtain a time-dependent model of slip and slip-rate with a non-negativity constraint applied to slip-rate [*Bartlow et al.*, 2011; *Miyazaki et al.*, 2006; *Segall and Matthews*, 1997]. Slip is assumed to occur on the plate interface (as defined by *McCrory et al.* [2012]) on a mesh of triangular dislocations in a homogenous elastic halfspace [*Thomas*, 1993]. Similar to the previous Oregon ETS event [*Bartlow et al.*, 2011], the results indicate a spatio-temporal correlation between high slip rate and the independently identified tremor epicenters for both ETS events (Figs. 2a and 3). And during the 3 weeks between events the model identifies 13 days of stationary, tremorless slip occurring with low slip speeds at the northern ETS initiation location.

The model also produces a spatiotemporal gap in slip and, having approached the lower resolution limits of the NIF model (Figs. S3-S6), it is unclear from GPS data whether slip migrated to this initiation point or the events remain separate. Slip duration from a moving source with low slip speeds could be too short to produce resolvable displacement. To address this question, we turn to borehole strainmeter data. Choosing the only two working stations near the gap ahead of the Oregon ETS slip front (Figs. 1 & 2), we compare the observed updip and downdip strain history with the tremor catalog and slip model (Fig. 2b). We focus on the ε_{ee}-ε_{nn} component of shear strain where positive and negative strain corresponds to extension and compression, respectively, in the strikeperpendicular direction. Both stations identify clear strain beginning between the two ETS events. The observed downdip extension and updip compression are consistent with reverse slip occurring in the tremor gap, and the first onset of strain on occurs on July 4 before the NIF identifies slip.

The presence of tremorless slip is also supported by the updip location of tremor after the gap (Fig. S1). Tremor from large and small events in Cascadia initiates deep and migrates updip prior to along-strike migration [*Wech and Creager*, 2011]. Tremor from the 2011 Washington ETS event, however, initiates at the updip edge of the ETS zone and immediately begins an along-strike migration, supporting the notion that updip slip was already underway.

We interpret the seismic, geodetic and strainmeter data to mean that low-level slip continued its northward migration from one ETS to another. This interpretation requires a tremorless continuation of low slip-rate slip that eventually stops migrating and accelerates in place prior to the Washington ETS event (Fig. 2).

Tremorless slip is observed elsewhere [*Brudzinski et al.*, 2010; *Hirose et al.*, 2010; *Ide*, 2012; *Ozawa et al.*, 2007; *Wallace et al.*, 2012] and its absence has been hypothesized to reflect differences in the rheological properties of the respective plate boundaries. The fact that a single event can alternate between tremor-genic and silent is therefore surprising. And what makes this observation truly remarkable is that we know this fault segment to be tremor-genic, so the absence of tremor cannot be explained by along-strike fault heterogeneity. Not only has this patch of fault generated tremor in prior ETS events (Fig. 4), it does so later within this same event as part of a back-propagating slip pulse (Figs. 1 & 2), and it even served as the initiation point for the 2009 ETS event [*Bartlow et al.*, 2011] (Fig. 4).

Physical models of tremorless slip

Understanding the connection between tremor and slip is fundamental to estimating the significance of tremor—or lack thereof—occurring adjacent to locked fault regions. The fact that slow

5

slip on some faults produces tremor while slow slip on other faults does not provides clues to the tremor generation process. But narrowing down the variables is difficult because the plate interface conditions and observational capabilities are different everywhere. By focusing on the same fault patch with the same instrumentation, we effectively have a controlled experiment and can limit our variables to what we can infer from the data. The observations show both a pause in along strike migration and a pronounced correlation between slip rate and tremor production. We propose a model in which tremor genesis is controlled by slip rate, and the slip rate and migration characteristics are controlled by local stress conditions.

We infer these relative local stress conditions from recent slip history. The tremor gap coincides with the segmentation boundary region between central and northern Cascadia. ETS recurs with 13-16-month intervals north of here and 20-month intervals south of here [*Brudzinski and Allen*, 2007], but events propagate to and sometimes through this boundary from either side. The previous northern ETS migrated through to the southern edge of the boundary (and observed gap) just 10.5 months prior (Fig. 4b). We suggest that when the 2011 central Cascadia ETS arrived at this boundary from the south, therefore, it encountered a fault segment that was not critically stressed and not ready to fully rupture.

Slip occurring in this under-stressed region would result in lower stress drops relative to large ETS-like slip. Because the ratio of propagation speed to slip speed is proportional to the peak-to-residual stress drop [*Ida*, 1973]

$$\frac{v_{\text{¿}}}{v_{slip}} = \alpha \frac{\mu}{\Delta\sigma_{p-r}}$$

where $v_{\text{¿}}$ is the migration velocity of the slip front, v_{slip} is the slip speed, μ is the shear modulus, α is constant that depends on the near-tip stress distribution, and $\Delta\sigma_{p-r}$ is the peak to residual shear stress, a combination of low stress-drop slip together with a stalled slip front unable to

6

advance could explain the decrease in slip speed (eg. *Rubin* [2011]). Eventually, this persistent, low slip-rate slip in the tremor gap stressed the adjacent Washington ETS fault segment to failure, and the high stress-drop failure resulted in an increase in slip rate, and the slow earthquake advanced along strike with typical ETS behavior.

Fluids are thought to play a major role in enabling slow slip to occur by reducing the effective stress with elevated pore pressures [*Audet et al.*, 2009]. A time-dependent pore pressure model could adjust the effective stress, thereby clamping and unclamping the fault, but there is no obvious mechanism for permeability or pore pressure changes on this timescale.

We prefer a model in which local stress conditions limit the slip rate, and the slip rate controls tremor genesis. It could be that asperity slip speed has a lower limit for tremor genesis or scales with tremor amplitude. Or perhaps there is a minimum required stressing rate required for asperity failure. Future studies involving low frequency earthquake production and detailed analysis of tremor amplitude may elucidate the exact mechanism, but what is clear is that slip here occurs with and without tremor depending on slip rate.

Conclusions

Our observations neither validate nor eliminate the above models, but our preferred model best explains the coincidence of tremor quiescence with low slip-rate, stationary slip and the subsequent secondary Washington ETS. The fact that we control for rheology does not rule it out entirely, especially since equally high or higher slip rate observed elsewhere is not necessarily co-located with detected tremor [*Brudzinski et al.*, 2010; *Hirose and Obara*, 2005; *Ozawa et al.*, 2007; *Wallace et al.*, 2012], but it does mean that site-specific rheologies alone cannot explain the occurrence of tremor. Based on our observations, slip speed and tremor rate are causally connected, but the slip rate, fault rheology, and stress conditions are all important factors in generating tremor.

7

Silent slip on a tremor-genic fault also means that the absence of tremor at other plate boundaries is not necessarily the result of data quality or undersampling. But perhaps a more important result is the effect such an observation has on our interpretation of observed tremor. While it is still likely true that tremor activity serves as a slip *indicator*, confirmed tremorless slip should discourage tremor's use as a slip *meter*. That is, *if tremor, then slip* is still true, but *if slip, then tremor* is not. In areas such as Cascadia, this means that tremor monitoring may not suffice for detecting transient events, tremor-based interpretations require caution, and discrepancies between tremor and slip distributions may be physical. This latter caveat is of particular interest in interpreting fault behavior closer to the seismogenic zone where slip distributions in Cascadia extend further updip than tremor [*Wech et al.*, 2009]. This updip region may be devoid of tremor asperities altogether. But if not, perhaps updip tremor asperities are even stronger than their ETS-zone counterparts and have not yet failed. Or the updip slip speed has so far been too slow to generate tremor. Either case emphasizes the need for routine monitoring, because updip tremor could signal even higher stresses transferred to the locked seismogenic zone.

Acknowledgments

We are grateful for discussion and suggestions from Paul Segall, Evelyn Roeloffs, Stephanie Prejean, and Joan Gomberg. We also thank Andrew Bradley and Yo Fukushima for contributing code used to invert geodetic data.

References

Audet, P., M. G. Bostock, N. I. Christensen, and S. M. Peacock (2009), Seismic evidence for overpressured subducted oceanic crust and megathrust fault sealing, *Nature*, *457*(7225), 76-78.

Bartlow, N. M., S. Miyazaki, A. M. Bradley, and P. Segall (2011), Space-time correlation of slip and tremor during the 2009 Cascadia slow slip event, *Geophysical Research Letters*, *38*(18), L18309.

 8

Bostock, M. G., A. A. Royer, E. H. Hearn, and S. M. Peacock (2012), Low frequency earthquakes below southern Vancouver Island, *Geochemistry Geophysics Geosystems*, *13*.

Brudzinski, M. R., and R. M. Allen (2007), Segmentation in episodic tremor and slip all along Cascadia, *Geology*, *35*(10), 907-910.

Brudzinski, M. R., H. R. Hinojosa-Prieto, K. M. Schlanser, E. CabralCano, A. Arciniega-Ceballos, O. Diaz-Molina, and C. DeMets (2010), Non-Volcanic tremor along the Oaxaca segment of the Middle America subduction Zone, *Journal of Geophysical Research-Solid Earth*, *115*, B00a23.

Hirose, H., and K. Obara (2005), Repeating short- and long-term slow slip events with deep tremor activity around the Bungo channel region, southwest Japan, *Earth Planets and Space*, *57*(10), 961-972.

Hirose, H., and K. Obara (2010), Recurrence behavior of short-term slow slip and correlated nonvolcanic tremor episodes in western Shikoku, southwest Japan, *Journal of Geophysical Research-Solid Earth*, *115*.

Hirose, H., Y. Asano, K. Obara, T. Kimura, T. Matsuzawa, S. Tanaka, and T. Maeda (2010), Slow Earthquakes Linked Along Dip in the Nankai Subduction Zone, *Science*, *330*(6010), 1502-1502.

Ida, Y. (1973), The maximum acceleration of seismic ground motion, *Bulletin of the Seismological Society of America*, *63*(3), 959-968.

Ide, S. (2012), Variety and spatial heterogeneity of tectonic tremor worldwide, *Journal of Geophysical Research*, *117*(B3).

Ito, Y., et al. (2013), Episodic slow slip events in the Japan subduction zone before the 2011 Tohoku-Oki earthquake, *Tectonophysics*, *600*, 14-26.

Kao, H., K. Wang, H. Dragert, J. Y. Kao, and G. Rogers (2010), Estimating seismic moment magnitude (Mw) of tremor bursts in northern Cascadia: Implications for the “seismic efficiency” of episodic tremor and slip, *Geophysical Research Letters*, *37*(19), n/a-n/a.

 9

Kato, A., K. Obara, T. Igarashi, H. Tsuruoka, S. Nakagawa, and N. Hirata (2012), Propagation of slow slip leading up to the 2011 M(w) 9.0 Tohoku-Oki earthquake, *Science*, *335*(6069), 705-708.

McCrory, P. A., J. L. Blair, F. Waldhauser, and D. H. Oppenheimer (2012), Juan de Fuca slab geometry and its relation to Wadati-Benioff zone seismicity, *Journal of Geophysical Research*, *117*(B9).

Miller, M. M., T. Melbourne, D. J. Johnson, and W. Q. Sumner (2002), Periodic slow earthquakes from the Cascadia subduction zone, *Science*, *295*, 2423.

Miyazaki, S. i., P. Segall, J. J. McGuire, T. Kato, and Y. Hatanaka (2006), Spatial and temporal evolution of stress and slip rate during the 2000 Tokai slow earthquake, *Journal of Geophysical Research*, *111*(B3).

Ozawa, S., H. Suito, T. Imakiire, and M. Murakmi (2007), Spatiotemporal evolution of aseismic interplate slip between 1996 and 1998 and between 2002 and 2004, in Bungo channel, southwest Japan, *Journal of Geophysical Research*, *112*(B5).

Peng, Z. G., and J. Gomberg (2010), An integrated perspective of the continuum between earthquakes and slow-slip phenomena, *Nature Geoscience*, *3*(9), 599-607.

Rogers, G., and H. Dragert (2003), Episodic tremor and slip on the Cascadia subduction zone: The chatter of silent slip, *Science*, *300*, 1942-1943.

Rubin, A. M. (2011), Designer friction laws for bimodal slow slip propagation speeds, *Geochemistry Geophysics Geosystems*, *12*(4).

Schwartz, S. Y., and J. M. Rokosky (2007), Slow slip events and seismic tremor at circum-pacific subduction zones, *Reviews of Geophysics*, *45*(3), RG3004.

Segall, P., and M. Matthews (1997), Time dependent inversion of geodetic data, *Journal of Geophysical Research*, *102*(B10), 22391-22409.

 10

Shelly, D. R., and K. M. Johnson (2011), Tremor reveals stress shadowing, deep postseismic creep, and depth-dependent slip recurrence on the lower-crustal San Andreas fault near Parkfield, *Geophysical Research Letters*, *38*(13), L13312.

Shelly, D. R., G. C. Beroza, and S. Ide (2007), Non-volcanic tremor and low-frequency earthquake swarms, *Nature*, *446*, 305-307.

Thomas, A. L. (1993), Poly3D: A three-dimensional, polygonal element, displacement discontinuity boundary element computer program with applications to fractures, faults, and cavities in the Earth's crust, Stanford University.

Wallace, L. M., J. Beavan, S. Bannister, and C. Williams (2012), Simultaneous long-term and short-term slow slip events at the Hikurangi subduction margin, New Zealand: Implications for processes that control slow slip event occurrence, duration, and migration, *Journal of Geophysical Research*, *117*(B11).

Wech, A. G. (2010), Interactive tremor monitoring, *Seismological Research Letters*, *81*(4), 664-669.

Wech, A. G., and K. C. Creager (2007), Cascadia tremor polarization evidence for plate interface slip, *Geophysical Research Letters*, *34*, L22306.

Wech, A. G., and K. C. Creager (2011), A continuum of stress, strength and slip in the Cascadia subduction zone, *Nature Geoscience*, *4*(9), 624-628.

Wech, A. G., K. C. Creager, and T. I. Melbourne (2009), Seismic and geodetic constraints on Cascadia slow slip, *Journal of Geophysical Research*, *114*, B10316, doi: 10.1029/2008jb006090.

Wech, A. G., K. C. Creager, H. Houston, and J. E. Vidale (2010), An earthquake-like magnitude-frequency distribution of slow slip in northern Cascadia, *Geophysical Research Letters*, *37*, L22310.

Wech, A. G., C. M. Boese, T. A. Stern, and J. Townend (2012), Tectonic tremor and deep slow slip on the Alpine Fault, *Geophysical Research Letters*, *39*(10), L10303, doi: 10.1029/2012gl051751.

 11

 12

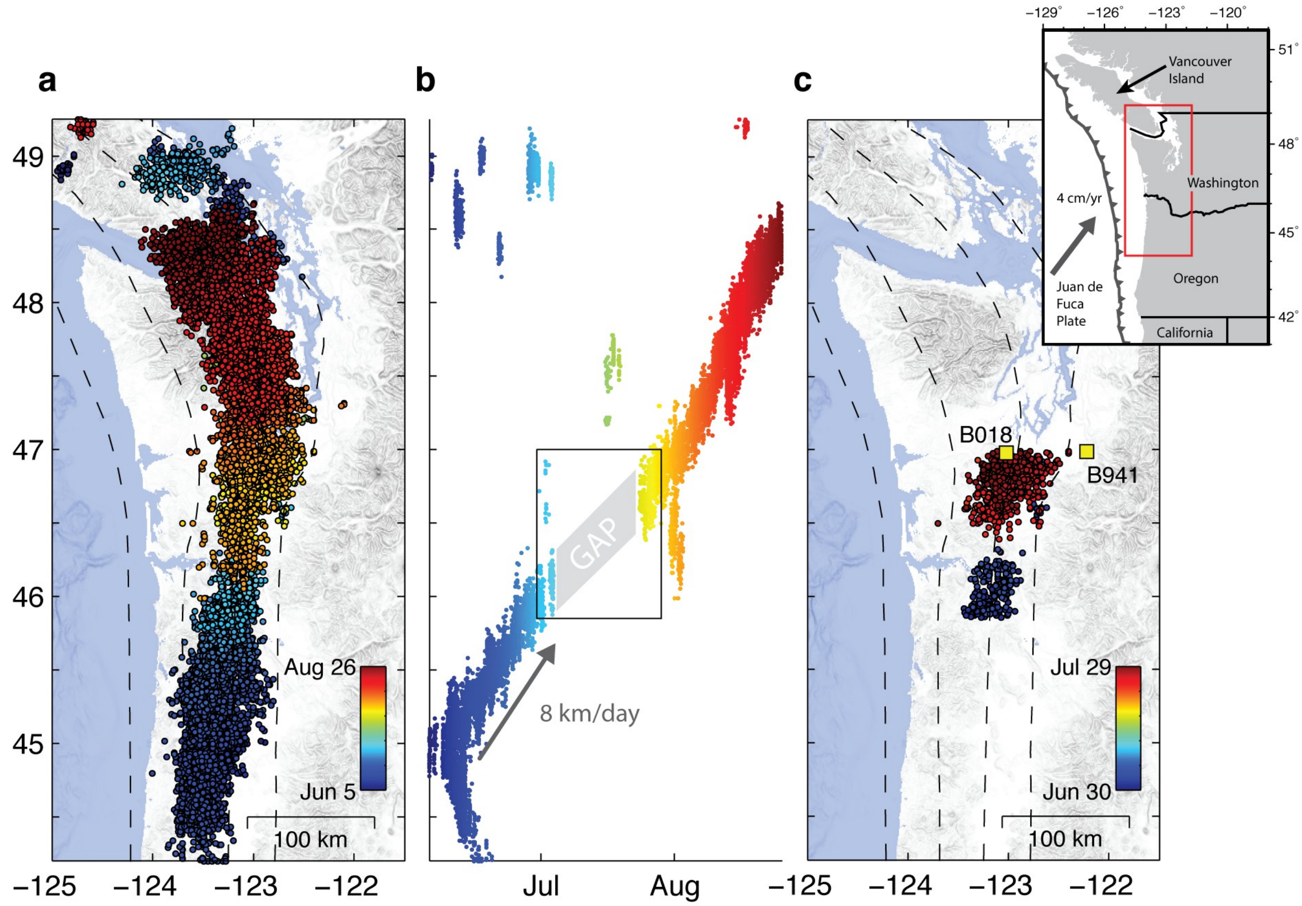

Figure 1 | Tremor migration pattern. a, Map of 2011 ETS color-coded tremor epicenters. **b**, Latitude vs. time of tremor epicenters color-coded with time range from left plot. **c**, Map of color-coded epicenters spatially and temporally limited to the rectangle from **b** surrounding the tremor gap. Yellow squares mark borehole strainmeters used in this study. Dashed lines mark 20-50km depth contours [*McCrory et al.*, 2012] (from left to right in 10km intervals). Upper right shows overview map and study area.

13

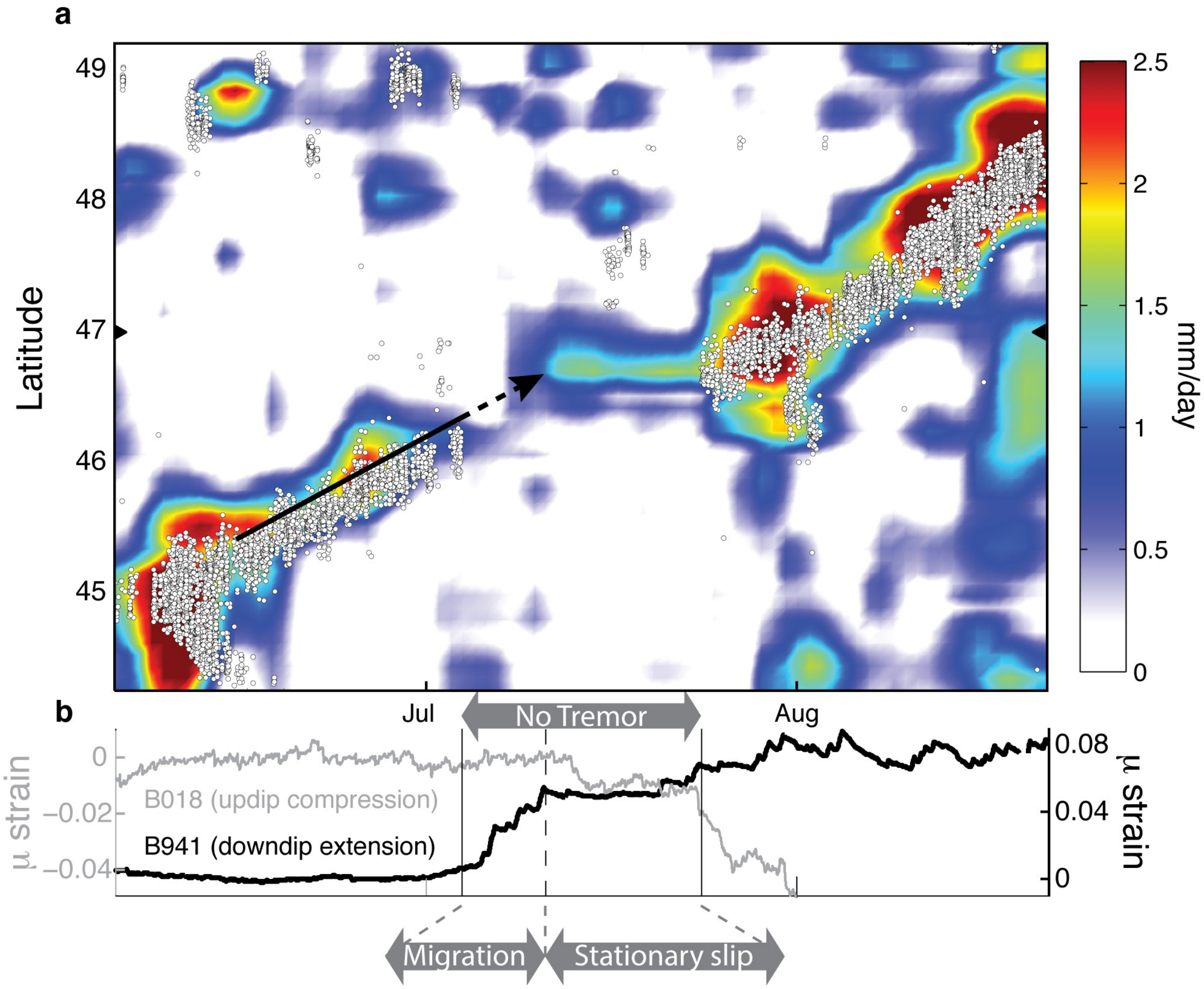

Figure 2 | Slip rate, tremor and strain. a, Latitude vs. time of slip rate from NIF (colors) and tremor epicenters (white circles). Latitude of strainmeters is shown by triangles on left and right axis. **b**, ε_{ee}-ε_{nn} strain component at B018 (grey, left axis) and B941 (black, right axis) with the < July 1 trend removed. Solid vertical lines surround the tremor gap. The dashed vertical line highlights change in strainmeter signal and beginning of low slip-rate slip identified in GPS. The flat portions of both strainmeter signals, while not completely understood, are consistent with the trends of previous ETS recordings in this area (Fig. S7). Note: B018 has data gap beginning on August 1.

 14

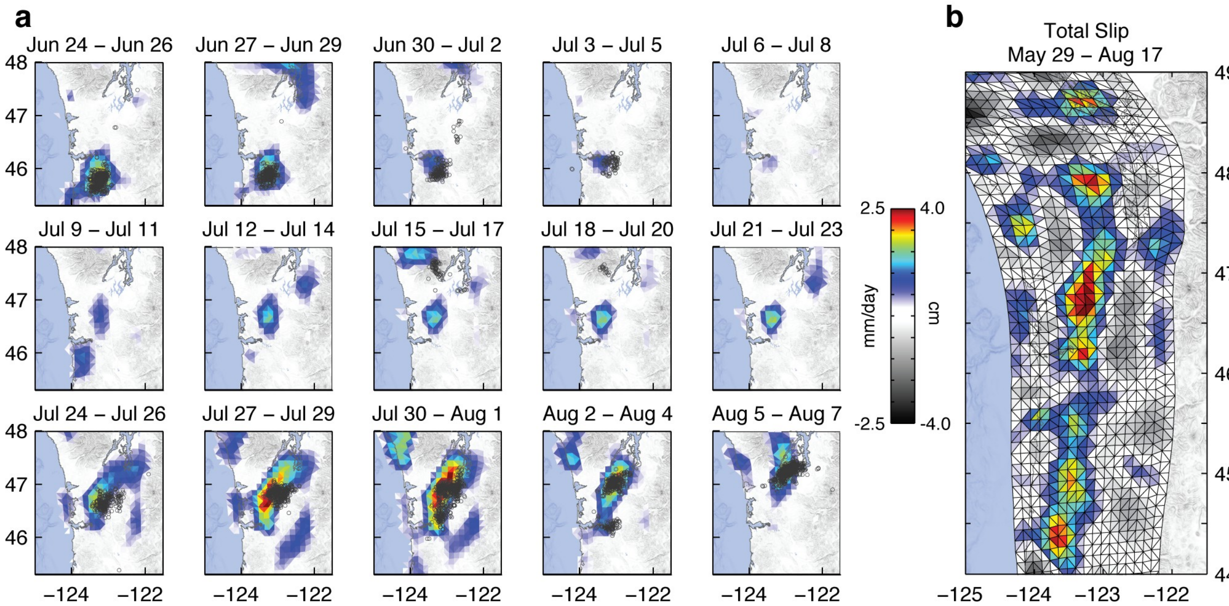

Figure 3 | Slip rate snapshots and total slip distribution. a, 3-day snapshots around gap time window from June 24 – August 8 of slip-rate (0 mm/day slip rate not plotted) and tremor (gray circles). **b**, resulting total slip from Network Inversion Filter. Colorbar represents slip rate for **a** in mm/day and the total slip for **b** in cm, respectively.

15

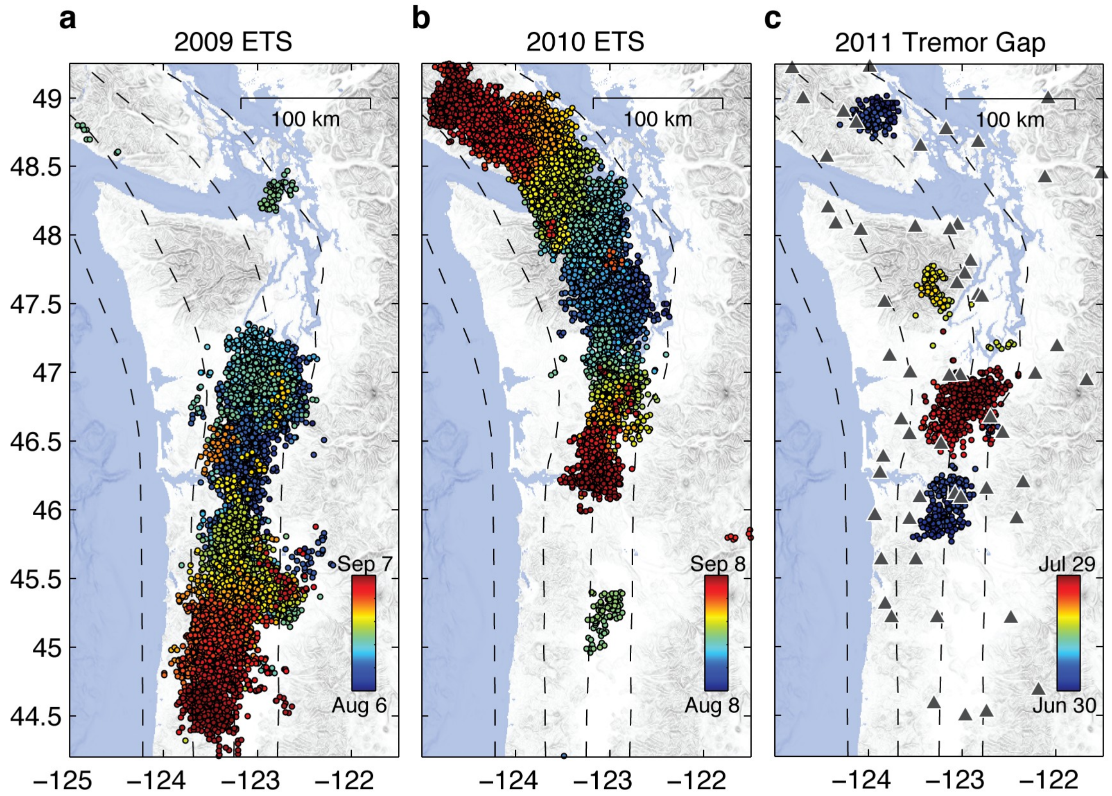

Figure 4 | Previous ETS gap tremor. Color-coded tremor epicenters of 2009 ETS event (**a**), 2010 ETS event (**b**), and the 2011 gap (**c**). Gray triangles in **c** mark seismic stations used in tremor detection [*Wech*, 2010]. Dashed lines mark 20-50km depth contours [*McCrory et al.*, 2012] (from left to right in 10km intervals).

16